

Accessing Chelating Extended Linker Bis(NHC) Palladium(II) Complexes: Sterically Triggered Divergent Reaction Pathways

Tanita S. Wierenga, Catriona R. Vanston, Alireza Ariaferd, Michael G. Gardiner, Curtis C. Ho*

School of Natural Sciences – Chemistry, University of Tasmania, Hobart, Tasmania, Australia

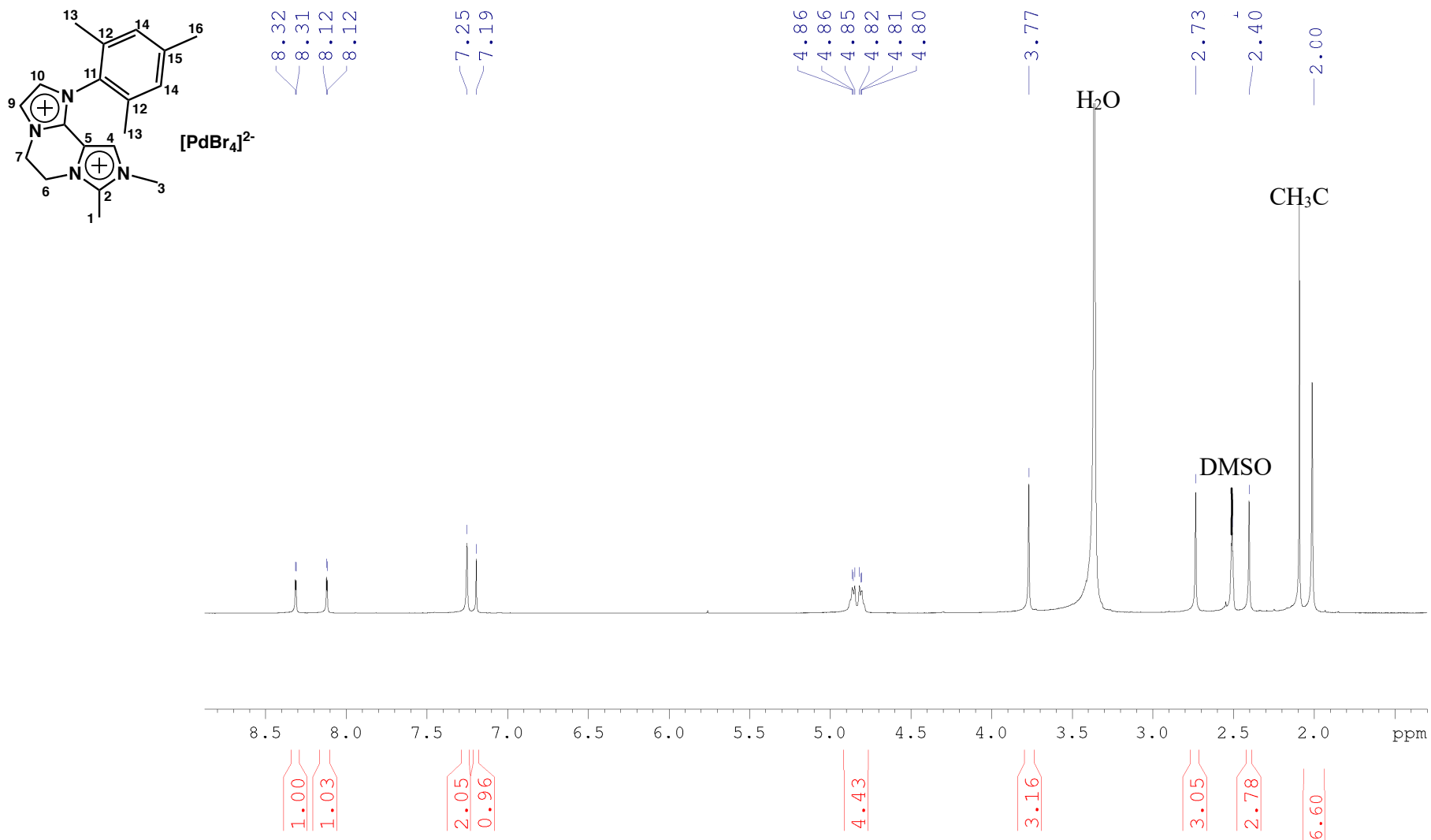
email: curtis.ho@utas.edu.au

Supporting Information

Table of Contents

I.	NMR spectra for compound VII	S-2
II.	X-Ray Crystallographic Data	S-4
III.	Density Functional Theory	S-9
IV.	References	S-13

I. NMR Spectra for Compound VII

MesIm)(1,2-Me₂Im-4H)C₂H₄][PdBr₄] (VII)**¹H NMR (DMSO-*d*₆, 400 MHz)****Figure S1** ¹H NMR spectrum of compound **VII** in DMSO-*d*₆

^{13}C NMR (DMSO- d_6 , 400 MHz)

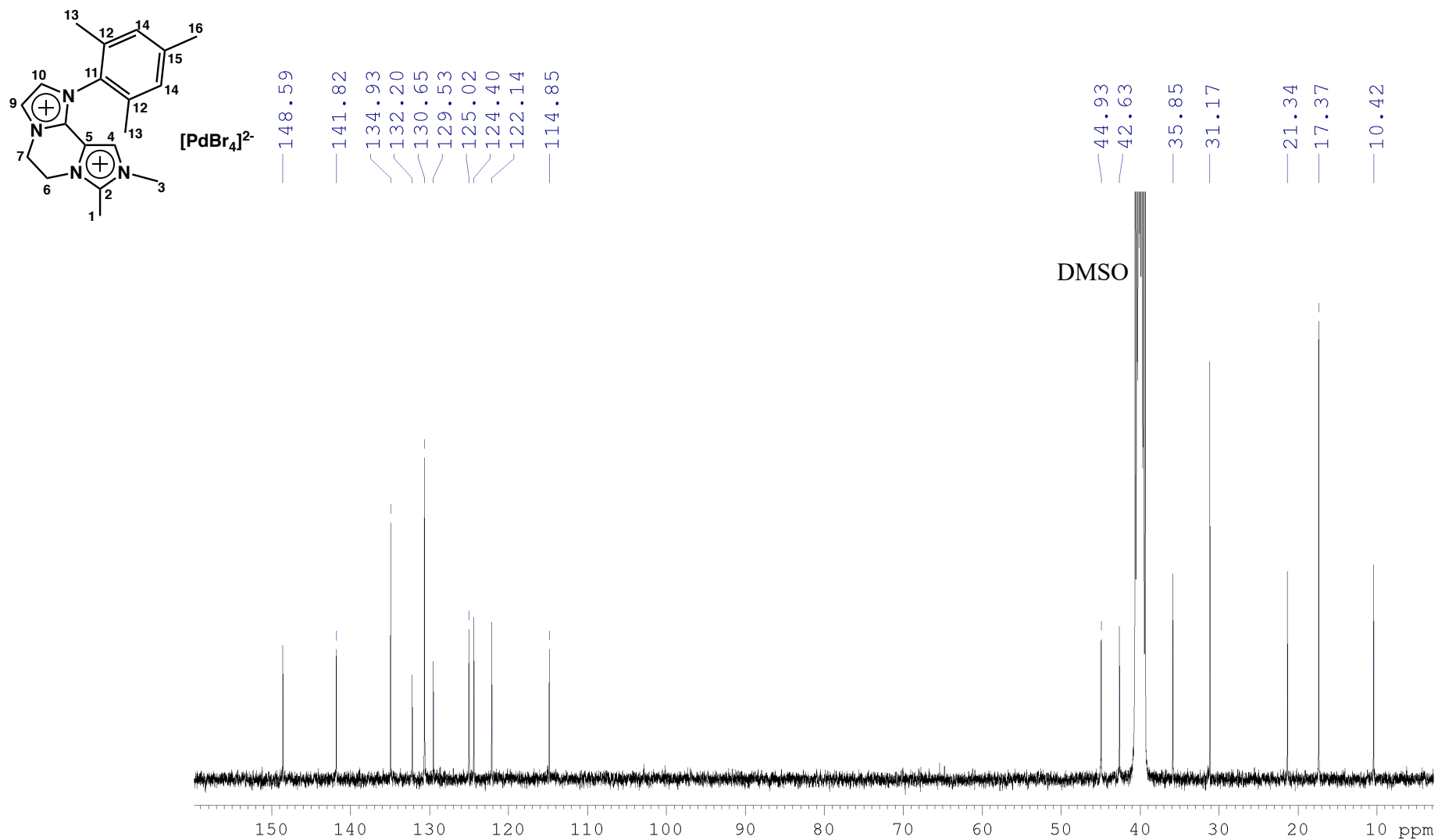


Figure S2 ^{13}C NMR spectrum of compound **VII** in DMSO- d_6

II. X-Ray Crystallographic Data

Crystallographic data for compounds **1a**, **1c**, **1la**, **1lb**, **1llb**, **1Vc**, **1V**, **1VI** and **1VII**.

Crystal data for compound **1a**: $C_{24}H_{28}N_4Br_2$, $M = 532.32$, orthorhombic, $a = 17.472(4)$, $b = 6.4620(13)$, $c = 21.226(4)$ Å, $U = 2396.5(8)$ Å³, $T = 100$ K, space group $Pna2_1$ (no. 33), $Z = 4$, 46094 reflections measured, 6990 unique ($R_{int} = 0.0662$), $5971 > 4\sigma(F)$, $R = 0.0522$ (observed), $R_w = 0.1461$ (all data). CCDC Number: 1915454

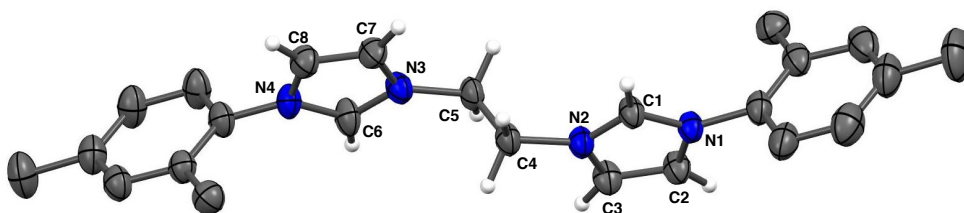


Figure S3. Structural representation of compound **1a**. Thermal ellipsoids are shown at 50% probability level. Br^- counteranions and N -substituent hydrogen atoms have been omitted for clarity

Crystal data for compound **1c**: $C_{34}H_{48}N_4Br_2Cl_4$, $M = 775.24$, triclinic, $a = 8.8660(18)$, $b = 9.4750(19)$, $c = 12.860(3)$ Å, $\alpha = 99.02(3)$, $\beta = 99.32(3)$, $\gamma = 113.93(3)^\circ$, $U = 944.3(4)$ Å³, $T = 100$ K, space group $P-1$ (no. 2), $Z = 1$, 15531 reflections measured, 4064 unique ($R_{int} = 0.0737$), $3440 > 4\sigma(F)$, $R = 0.0751$ (observed), $R_w = 0.2208$ (all data). CCDC Number: 1915452

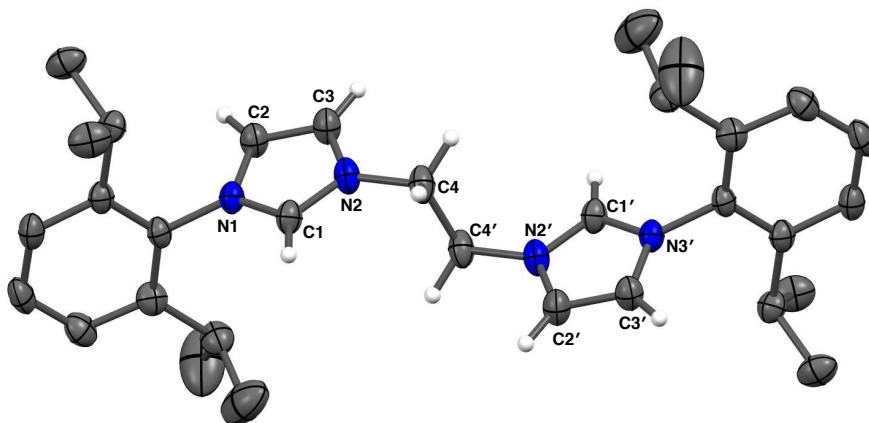


Figure S4. Structural representation of compound **1c** (' denotes symmetry operator: $-x, -y, -z$). Thermal ellipsoids are shown at 50% probability level. Br^- counteranions, lattice CH_2Cl_2 solvent molecules and N -substituent hydrogen atoms have been omitted for clarity.

Crystal data for compound **IIa**: $C_{24}H_{26}Br_2N_4Pd$, $M = 636.71$, triclinic, $a = 7.9690(16)$, $b = 15.138(3)$, $c = 19.963(4)$ Å, $\alpha = 89.51(3)$, $\beta = 89.98(3)$, $\gamma = 83.31(3)$ °, $U = 2391.8(8)$ Å³, $T = 100$ K, space group $P\bar{1}$ (no 2), $Z = 4$, 50914 reflections measured, 13311 unique ($R_{int} = 0.1154$), 10264 $> 4\sigma(F)$, $R = 0.0566$ (observed), $R_w = 0.1546$ (all data). CCDC Number: 1915457

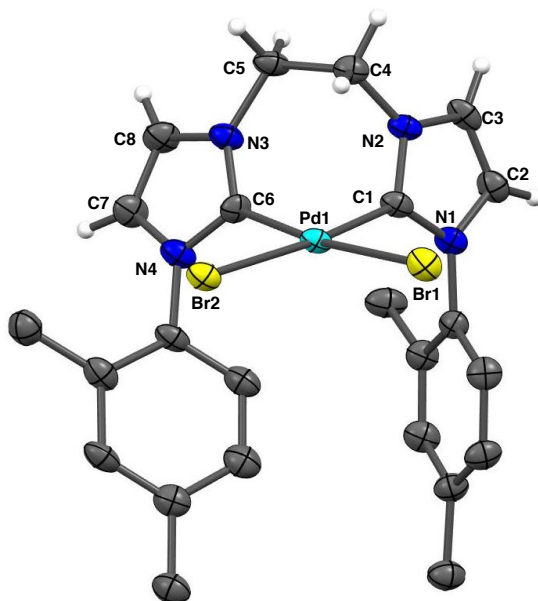


Figure S5. Structural representation of compound **IIa**. Thermal ellipsoids are shown at 50% probability level. *N*-substituent hydrogen atoms have been omitted for clarity. Selected bond lengths (Å) and angles (°): Pd1-C1,C6 1.973(6), 1.977(5), Pd1-Br1,Br2 2.477(1), 2.504(1), C1-Pd1-C6 85.5(2), Br1-Pd1-Br2 94.91(2), Pd1-C1-N2 120.6(4), Pd1-C6-N3 127.6(4) .

Crystal data for complex **IIb**: $C_{27}H_{32}Br_2Cl_2N_4Pd$, $M = 749.68$, monoclinic, $a = 11.631(3)$, $b = 14.050(9)$, $c = 17.964(2)$ Å, $\alpha = 90$, $\beta = 99.88(7)$, $\gamma = 90$ °, $U = 2982.1(10)$ Å³, $T = 100$ K, space group $P2_1/n$ (no. 14), $Z = 4$, 43671 reflections measured, 6345 unique ($R_{int} = 0.0347$), 6204 $> 4\sigma(F)$, $R = 0.0795$ (observed), $R_w = 0.2145$ (all data). CCDC Number: 1915459

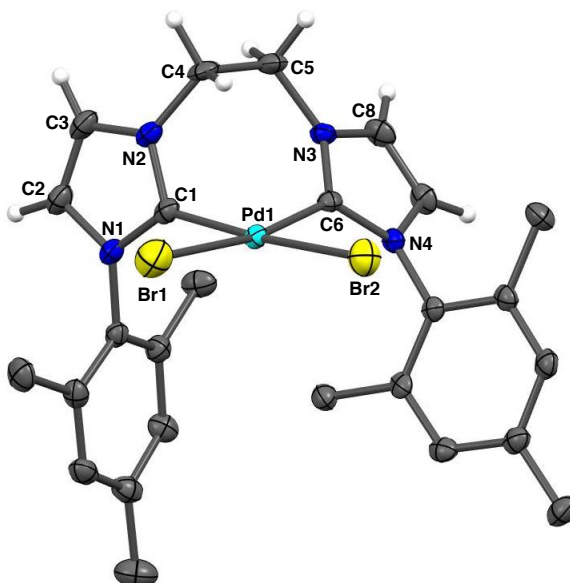


Figure S6. Structural representation of complex **IIb**. Thermal ellipsoids are shown at 50% probability level. Lattice CH₂Cl₂ solvent molecules and *N*-substituent hydrogen atoms have been omitted for clarity. Selected bond lengths (Å) and angles (°): Pd1-C1, C6 2.002(7), 1.992(7), Pd1-Br1, Br2 2.4996(13), 2.4907(12), C1-Pd1-C6 87.5(3), Br1-Pd1-Br2 90.66(4)

Crystal data for complex **IIIb**: C₂₆H₂₉Br₃N₄Pd, *M* = 743.67, monoclinic, *a* = 16.659(3), *b* = 11.386(2), *c* = 17.142(3) Å, β = 104.31(3)°, *U* = 3150.7(12) Å³, *T* = 100 K, space group P2₁/*n* (no. 14), *Z* = 4, 48236 reflections measured, 6952 unique (*R*_{int} = 0.0496), 5715 > 4σ(*F*), *R* = 0.0395 (observed), *R*_w = 0.1003 (all data). CCDC Number: 1915458

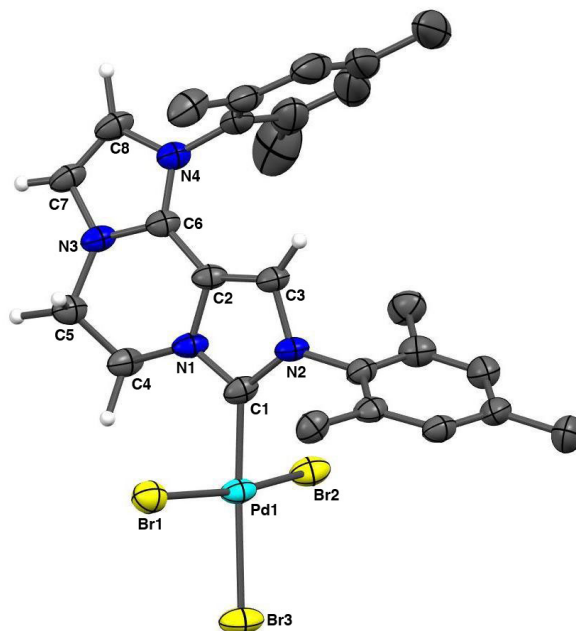


Figure S7. Structural representation of complex **IIIb**. Thermal ellipsoids are shown at 50% probability level. *N*-substituent hydrogen atoms have been omitted for clarity. Selected bond lengths (Å) and angles (°): Pd1-C1 1.954(4), Pd1-Br1, Br2, Br3 2.4497(8), 2.4914(8), 2.4451(8), C1-Pd1-Br1, Br3 89.19(14), 85.57(14), Br1-Pd1-Br2 90.59(3), Br2-Pd1-Br3 95.35(3).

Crystal data for complex **IVc**: $C_{33.79}H_{45.6825}Br_3N_{4.895}Pd$, $M = 866.57$, triclinic, $a = 10.417(2)$, $b = 13.912(3)$, $c = 27.084(5)$ Å, $\alpha = 83.16(3)$, $\beta = 79.93(3)$, $\gamma = 74.26(3)$ ° $U = 3709.1(15)$ Å³, $T = 100$ K, space group $P-1$ (no. 2), $Z = 4$, 62580 reflections measured, 16270 unique ($R_{int} = 0.1123$), $10207 > 4\sigma(F)$, $R = 0.0701$ (observed), $R_w = 0.2004$ (all data). CCDC Number: 1915453

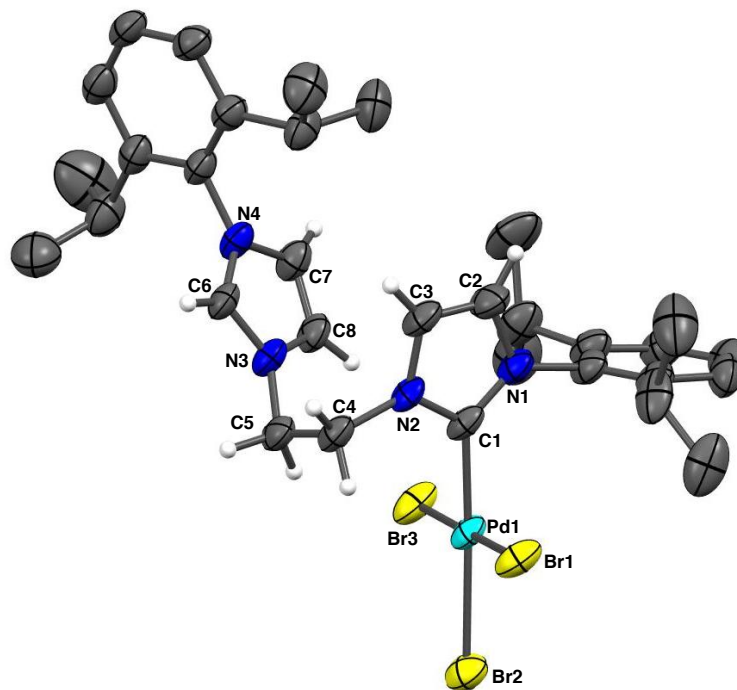


Figure S8. Structural representation of complex **IVc**. Thermal ellipsoids are shown at 50% probability level. *N*-substituent hydrogen atoms have been omitted for clarity. Selected bond lengths (Å) and angles (°): Pd1-C1 1.993(1), Pd1-Br1,Br2,Br3 2.429(1), 2.518(1), 2.424(1), C1-Pd1-Br1,Br3 86.1(2), 92.4(2), Br1-Pd1-Br1,Br3 92.63(3), 88.82(4).

Crystal data for compound **VI**: $C_{19}H_{26}Br_2N_4$, $M = 470.26$, monoclinic, $a = 10.451(2)$, $b = 8.0570(16)$, $c = 24.629(5)$ Å, $\beta = 101.11(3)^\circ$, $U = 2035.0(7)$ Å³, $T = 100$ K, space group $P12_1/c_1$ (no. 14), $Z = 4$, 33377 reflections measured, 4567 unique ($R_{\text{int}} = 0.0384$), $3924 > 4\sigma(F)$, $R = 0.0427$ (observed), $R_w = 0.1124$ (all data). CCDC Number: 1915455

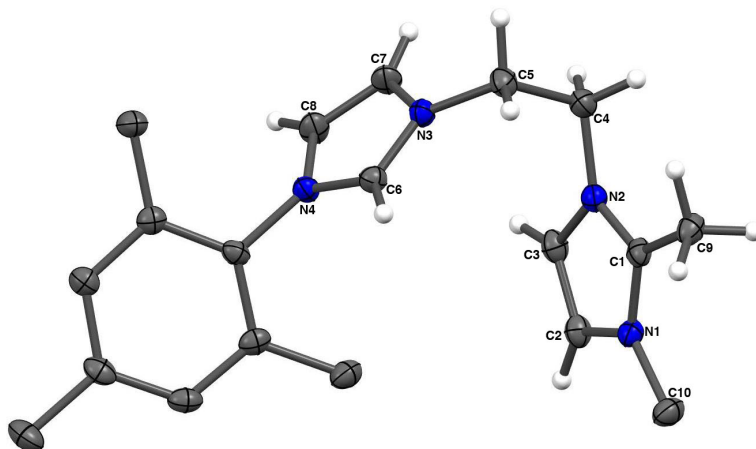


Figure S9. Structural representation of compound **VI**. Thermal ellipsoids are shown at 50% probability level. Br^- counteranions and N -substituent hydrogen atoms have been omitted for clarity. Selected bond lengths (Å) and angles ($^\circ$): C1-C9 1.479(5), N1-C1-C9 125.3(3), N2-C1-C9 125.3(3).

Crystal data for compound **VII**: $C_{21}H_{27}Br_4N_5Pd$, $M = 775.51$, monoclinic, $a = 19.980(4)$, $b = 8.0800(16)$, $c = 16.845(3)$ Å, $\beta = 103.24(3)^\circ$, $U = 2647.2(10)$ Å³, $T = 100$ K, space group $C121$ (no. 5), $Z = 4$, 22260 reflections measured, 6256 unique ($R_{\text{int}} = 0.1044$), $4454 > 4\sigma(F)$, $R = 0.0684$ (observed), $R_w = 0.1815$ (all data). CCDC Number: 1915456

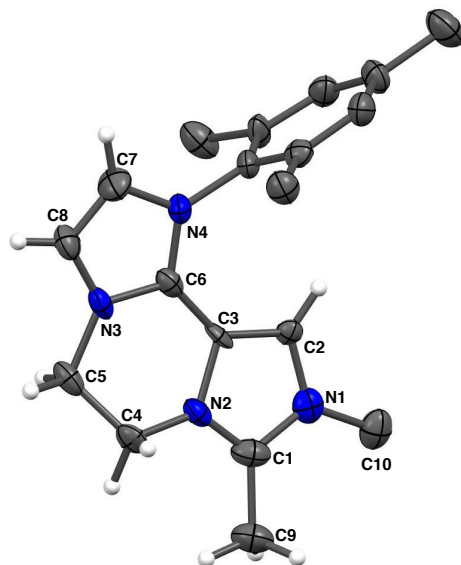


Figure S10. Structural representation of compound **VII**. Thermal ellipsoids are shown at 50% probability level. $[PdBr_4]^{2-}$ counteranion, lattice acetonitrile solvent molecules and N -substituent hydrogen atoms have been omitted for clarity. Selected bond lengths (Å) and angles ($^\circ$): C1-C9 1.501(3), C3-C6 1.417(2), N1-C1-C9 124.92(1), N2-C1-C9 126.29(1), N2-C3-C6 117.08(1), N4-C6-C3 130.30(1), C2-C3-C6 135.98(1).

II. Density Functional Theory Computational Data

Table S1. Total energies for all of the calculated structures

1

E (B3LYP/BS1, Solvent = DiMethylSulfoxide) = -6726.643269 au
 H(B3LYP/BS1, Solvent = DiMethylSulfoxide) = -6726.024656 au
 G(B3LYP/BS1, Solvent = DiMethylSulfoxide) = -6726.144782 au
 E(B3LYP/BS2//B3LYP/BS1, Solvent = DiMethylSulfoxide) = -6733.782326 au
 E(M06/BS2//B3LYP/BS1, Solvent = DiMethylSulfoxide) = -6732.420723 au

2

E (B3LYP/BS1, Solvent = DiMethylSulfoxide) = -6726.629585 au
 H(B3LYP/BS1, Solvent = DiMethylSulfoxide) = -6726.011068 au
 G(B3LYP/BS1, Solvent = DiMethylSulfoxide) = -6726.130683 au
 E(B3LYP/BS2//B3LYP/BS1, Solvent = DiMethylSulfoxide) = -6733.769807 au
 E(M06/BS2//B3LYP/BS1, Solvent = DiMethylSulfoxide) = -6732.411312 au

3

E (B3LYP/BS1, Solvent = DiMethylSulfoxide) = -4155.037211 au
 H(B3LYP/BS1, Solvent = DiMethylSulfoxide) = -4154.421327 au
 G(B3LYP/BS1, Solvent = DiMethylSulfoxide) = -4154.536051 au
 E(B3LYP/BS2//B3LYP/BS1, Solvent = DiMethylSulfoxide) = -4159.430358 au
 E(M06/BS2//B3LYP/BS1, Solvent = DiMethylSulfoxide) = -4158.195471 au

Br⁻

E (B3LYP/BS1, Solvent = DiMethylSulfoxide) = -2571.574251 au
 H(B3LYP/BS1, Solvent = DiMethylSulfoxide) = -2571.57189 au
 G(B3LYP/BS1, Solvent = DiMethylSulfoxide) = -2571.590426 au
 E(B3LYP/BS2//B3LYP/BS1, Solvent = DiMethylSulfoxide) = -2574.334887 au
 E(M06/BS2//B3LYP/BS1, Solvent = DiMethylSulfoxide) = -2574.192852 au

TS₃₋₄

E (B3LYP/BS1, Solvent = DiMethylSulfoxide) = -4154.998951 au
 H(B3LYP/BS1, Solvent = DiMethylSulfoxide) = -4154.387613 au
 G(B3LYP/BS1, Solvent = DiMethylSulfoxide) = -4154.497913 au
 E(B3LYP/BS2//B3LYP/BS1, Solvent = DiMethylSulfoxide) = -4159.389883 au
 E(M06/BS2//B3LYP/BS1, Solvent = DiMethylSulfoxide) = -4158.168610 au

4

E (B3LYP/BS1, Solvent = DiMethylSulfoxide) = -4155.034072 au
 H(B3LYP/BS1, Solvent = DiMethylSulfoxide) = -4154.417272 au
 G(B3LYP/BS1, Solvent = DiMethylSulfoxide) = -4154.530056 au
 E(B3LYP/BS2//B3LYP/BS1, Solvent = DiMethylSulfoxide) = -4159.427097 au
 E(M06/BS2//B3LYP/BS1, Solvent = DiMethylSulfoxide) = -4158.208287 au

HOAc

E (B3LYP/BS1, Solvent = DiMethylSulfoxide) = -229.0841903 au
 H(B3LYP/BS1, Solvent = DiMethylSulfoxide) = -229.016870 au
 G(B3LYP/BS1, Solvent = DiMethylSulfoxide) = -229.049876 au
 E(B3LYP/BS2//B3LYP/BS1, Solvent = DiMethylSulfoxide) = -229.1773463 au

E(M06/BS2//B3LYP/BS1, Solvent = DiMethylSulfoxide) = -229.0428887 au

IIb

E (B3LYP/BS1, Solvent = DiMethylSulfoxide) = -6497.533325 au

H(B3LYP/BS1, Solvent = DiMethylSulfoxide) = -6496.983482 au

G(B3LYP/BS1, Solvent = DiMethylSulfoxide) = -6497.089445 au

E(B3LYP/BS2//B3LYP/BS1, Solvent = DiMethylSulfoxide) = -6504.587073 au

E(M06/BS2//B3LYP/BS1, Solvent = DiMethylSulfoxide) = -6503.367574 au

TS_{IIb-5}

E (B3LYP/BS1, Solvent = DiMethylSulfoxide) = -6497.463818 au

H(B3LYP/BS1, Solvent = DiMethylSulfoxide) = -6496.916318 au

G(B3LYP/BS1, Solvent = DiMethylSulfoxide) = -6497.021610 au

E(B3LYP/BS2//B3LYP/BS1, Solvent = DiMethylSulfoxide) = -6504.513993 au

E(M06/BS2//B3LYP/BS1, Solvent = DiMethylSulfoxide) = -6503.304191 au

5

E (B3LYP/BS1, Solvent = DiMethylSulfoxide) = -6497.484825 au

H(B3LYP/BS1, Solvent = DiMethylSulfoxide) = -6496.93521 au

G(B3LYP/BS1, Solvent = DiMethylSulfoxide) = -6497.04155 au

E(B3LYP/BS2//B3LYP/BS1, Solvent = DiMethylSulfoxide) = -6504.531484 au

E(M06/BS2//B3LYP/BS1, Solvent = DiMethylSulfoxide) = -6503.333456 au

TS₃₋₆

E (B3LYP/BS1, Solvent = DiMethylSulfoxide) = -4155.002023 au

H(B3LYP/BS1, Solvent = DiMethylSulfoxide) = -4154.390321 au

G(B3LYP/BS1, Solvent = DiMethylSulfoxide) = -4154.504281 au

E(B3LYP/BS2//B3LYP/BS1, Solvent = DiMethylSulfoxide) = -4159.396974 au

E(M06/BS2//B3LYP/BS1, Solvent = DiMethylSulfoxide) = -4158.165245 au

6

E (B3LYP/BS1, Solvent = DiMethylSulfoxide) = -4155.037687 au

H(B3LYP/BS1, Solvent = DiMethylSulfoxide) = -4154.421085 au

G(B3LYP/BS1, Solvent = DiMethylSulfoxide) = -4154.539709 au

E(B3LYP/BS2//B3LYP/BS1, Solvent = DiMethylSulfoxide) = -4159.432364 au

E(M06/BS2//B3LYP/BS1, Solvent = DiMethylSulfoxide) = -4158.20112 au

TS₇₋₈

E (B3LYP/BS1, Solvent = DiMethylSulfoxide) = -4154.997825 au

H(B3LYP/BS1, Solvent = DiMethylSulfoxide) = -4154.383230 au

G(B3LYP/BS1, Solvent = DiMethylSulfoxide) = -4154.500969 au

E(B3LYP/BS2//B3LYP/BS1, Solvent = DiMethylSulfoxide) = -4159.388634 au

E(M06/BS2//B3LYP/BS1, Solvent = DiMethylSulfoxide) = -4158.169080 au

7

E (B3LYP/BS1, Solvent = DiMethylSulfoxide) = -6497.536145 au

H(B3LYP/BS1, Solvent = DiMethylSulfoxide) = -6496.986118 au

G(B3LYP/BS1, Solvent = DiMethylSulfoxide) = -6497.096433 au

E(B3LYP/BS2//B3LYP/BS1, Solvent = DiMethylSulfoxide) = -6504.591777 au

E(M06/BS2//B3LYP/BS1, Solvent = DiMethylSulfoxide) = -6503.360605 au

10

E (B3LYP/BS1, Solvent = DiMethylSulfoxide) = -4155.035824 au
H(B3LYP/BS1, Solvent = DiMethylSulfoxide) = -4154.419086 au
G(B3LYP/BS1, Solvent = DiMethylSulfoxide) = -4154.53718 au
E(B3LYP/BS2//B3LYP/BS1, Solvent = DiMethylSulfoxide) = -4159.424799 au
E(M06/BS2//B3LYP/BS1, Solvent = DiMethylSulfoxide) = -4158.209986 au

9

E (B3LYP/BS1, Solvent = DiMethylSulfoxide) = -3925.92642 au
H(B3LYP/BS1, Solvent = DiMethylSulfoxide) = -3925.378951 au
G(B3LYP/BS1, Solvent = DiMethylSulfoxide) = -3925.482678 au
E(B3LYP/BS2//B3LYP/BS1, Solvent = DiMethylSulfoxide) = -3930.237161 au
E(M06/BS2//B3LYP/BS1, Solvent = DiMethylSulfoxide) = -3929.130504 au

8

E (B3LYP/BS1, Solvent = DiMethylSulfoxide) = -6497.532579 au
H(B3LYP/BS1, Solvent = DiMethylSulfoxide) = -6496.983249 au
G(B3LYP/BS1, Solvent = DiMethylSulfoxide) = -6497.089835 au
E(B3LYP/BS2//B3LYP/BS1, Solvent = DiMethylSulfoxide) = -6504.583353 au
E(M06/BS2//B3LYP/BS1, Solvent = DiMethylSulfoxide) = -6503.367654 au

11

E (B3LYP/BS1, Solvent = DiMethylSulfoxide) = -3925.936520 au
H(B3LYP/BS1, Solvent = DiMethylSulfoxide) = -3925.388417 au
G(B3LYP/BS1, Solvent = DiMethylSulfoxide) = -3925.490384 au
E(B3LYP/BS2//B3LYP/BS1, Solvent = DiMethylSulfoxide) = -3930.240865 au
E(M06/BS2//B3LYP/BS1, Solvent = DiMethylSulfoxide) = -3929.153446 au

TS₉₋₁₁

E (B3LYP/BS1, Solvent = DiMethylSulfoxide) = -3925.898613 au
H(B3LYP/BS1, Solvent = DiMethylSulfoxide) = -3925.352545 au
G(B3LYP/BS1, Solvent = DiMethylSulfoxide) = -3925.453324 au
E(B3LYP/BS2//B3LYP/BS1, Solvent = DiMethylSulfoxide) = -3930.205896 au
E(M06/BS2//B3LYP/BS1, Solvent = DiMethylSulfoxide) = -3929.111058 au

TS₇₋₈

E (B3LYP/BS1, Solvent = DiMethylSulfoxide) = -6497.492139 au
H(B3LYP/BS1, Solvent = DiMethylSulfoxide) = -6496.944052 au
G(B3LYP/BS1, Solvent = DiMethylSulfoxide) = -6497.052391 au
E(B3LYP/BS2//B3LYP/BS1, Solvent = DiMethylSulfoxide) = -6504.545011 au
E(M06/BS2//B3LYP/BS1, Solvent = DiMethylSulfoxide) = -6503.323169 au

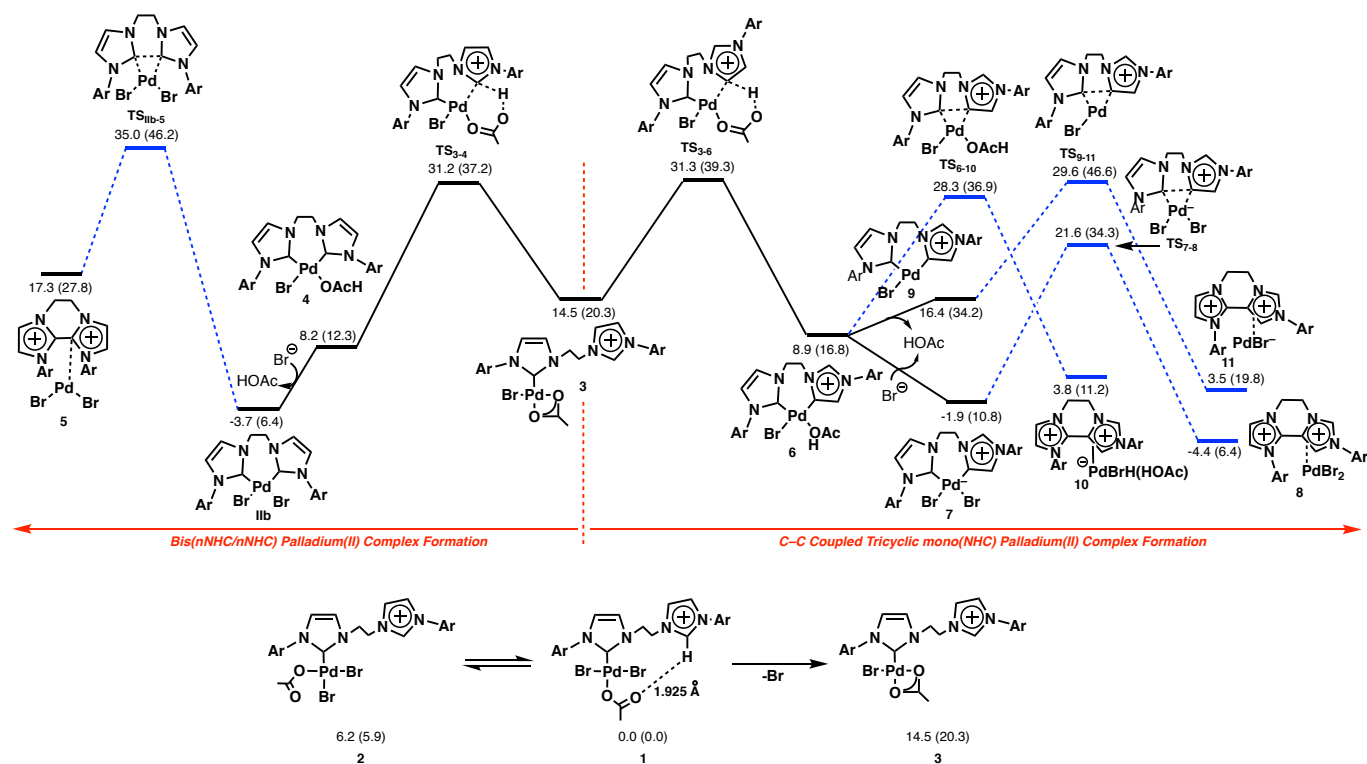


Figure S11. Energy profile calculated for the formation of abnormal and normal carbenes promoted by Pd^{II}. The relative Gibbs and electronic energies (in parentheses) obtained from the M06/BS2//B3LYP/BS1 calculations in dimethylsulfoxide are given in kcal/mol.

Computational details: Gaussian 09¹ was used to fully optimize all the structures reported in this paper at the B3LYP level of density functional theory (DFT) in dimethylsulfoxide using the CPCM solvation model.^{2,3} The effective-core potential of Hay and Wadt with a double- ξ valence basis set (LANL2DZ)⁴ was chosen to describe Pd. The 6-31G(d) basis set was used for other atoms.⁵ A Polarization function of $\xi_f = 1.472$ were also added for Pd.⁶ This basis set combination will be referred to as BS1. Frequency calculations were carried out at the same level of theory as those for the structural optimization. Transition states were located using the Berny algorithm. Intrinsic reaction coordinate (IRC)⁷ calculations were used to confirm the connectivity between transition structures and minima. To further refine the energies obtained from the B3LYP/BS1 calculations, we carried out single-point energy calculations for all of the structures with a larger basis set (BS2) at the B3LYP and M06⁸ levels with inclusion of the solvent effect. BS2 utilizes the quadruple- ζ valence def2-QZVP⁹ basis set on Pd and the 6-311+G(2d,p) basis set on other atoms. We have used the potential and Gibbs free energies obtained from the M06/BS2//B3LYP/BS1 calculations in dimethylsulfoxide throughout the paper unless otherwise stated. The atomic orbital populations were calculated on the basis of natural bond orbital (NBO) analyses.¹⁰

IV. References

1. Frisch, M. J.; *et al.* Gaussian 09, revision A.02; Gaussian, Inc.: Wallingford, CT, 2009.
2. Barone, V.; Cossi, M. Quantum Calculation of Molecular Energies and Energy Gradients in Solution by a Conductor Solvent Model. *J. Phys. Chem. A*. **1998**, *102*, 1995–2001.
3. (a) Lee, C. T.; Yang, W. T.; Parr, R. G. Development of the Colle-Salvetti correlation-energy formula into a functional of the electron density. *Phys. Rev. B*. **1988**, *37*, 785; (b) Miehlich, B.; Savin, A.; Stoll, H.; Preuss, H. Results obtained with the correlation energy density functionals of Becke and Lee, Yang and Parr. *Chem. Phys. Lett.* **1989**, *157*, 200–206; (c) Becke, A. D. Density-functional thermochemistry. III. The role of exact exchange. *J. Chem. Phys.* **1993**, *98*, 5648.
4. (a) Hay, P. J.; Wadt, W. R. *Ab initio* effective core potentials for molecular calculations. Potentials for the transition metal atoms Sc to Hg. *J. Chem. Phys.* **1985**, *82*, 270; (b) Wadt, W. R.; Hay, P. J. *Ab initio* effective core potentials for molecular calculations. Potentials for main group elements Na to Bi. *J. Chem. Phys.* **1985**, *82*, 284.
5. Hariharan, P. C.; Pople, J. A. The influence of polarization functions on molecular orbital hydrogenation energies. *Theor. Chim. Acta* **1973**, *28*, 213–222.
6. (a) Ehlers, A. W.; Böhme, M.; Dapprich, S.; Gobbi, A.; Höllwarth, A.; Jonas, V.; Köhler, K. F.; Stegmann, R.; Veldkamp, A.; Frenking, G. A set of f-polarization functions for pseudo-potential basis sets of the transition metals Sc→Cu, Y→Ag and La→Au. *Chem. Phys. Lett.* **1993**, *208*, 111–114; (b) Höllwarth, A.; Böhme, M.; Dapprich, S.; Ehlers, A. W.; Gobbi, A.; Jonas, V.; Köhler, K. F.; Stegmann, R.; Veldkamp, R. A.; Frenking, G. A set of d-polarization functions for pseudo-potential basis sets of the main elements Al→Bi and f-type polarization functions for Zn, Cd, Hg. *Chem. Phys. Lett.* **1993**, *208*, 237–240.
7. (a) Fukui, K. Formulation of the reaction coordinate. *J. Phys. Chem.* **1970**, *74*, 4161–4163; (b) Fukui, K. The path of chemical reactions – the IRC approach. *Acc. Chem. Res.* **1981**, *14*, 363–368.
8. Zhao, Y.; Truhlar, D. G. Density Functionals with Broad Applicability in Chemistry. *Acc. Chem. Res.* **2008**, *41*, 157–167.
9. Weigend, F.; Furche, F.; Ahlrichs, R. Gaussian basis sets of quadruple zeta valence quality for atoms H-Kr. *J. Chem. Phys.* **2003**, *119*, 12753.
10. Glendening, E. D.; Read, A. E.; Carpenter, J. E.; Weinhold, F. NBO, version 3.1; Gaussian, Inc.: Pittsburgh, PA, **2003**.